

Dopplerson-phonon resonance in cadmium

S. V. Medvedev, V. G. Skobov, L. M. Fisher, and V. A. Yudin

V. I. Lenin All-Union Electrotechnical Institute

(Submitted August 7, 1975)

Zh. Eksp. Teor. Fiz. 69, 2267-2279 (December 1975)

The resonance interaction between a dopplerson wave and a sound wave in cadmium located in a magnetic field parallel to the hexagonal axis is investigated. A theory of the dopplerson-phonon resonance is constructed which takes into account the induction, as well as the deformation interaction of the electrons with the lattice vibrations. The effect of the resonance on the properties of the dopplerson and the sound wave is studied. It is shown that the attenuation of both waves is maximal in the resonance region. The oscillations of the surface resistance of a cadmium plate located in a magnetic field $\mathbf{H} \parallel [0001]$ is experimentally studied in the 25-100 MHz frequency range. It is found that in the region of field intensities corresponding to the dopplerson-phonon resonance the amplitude of the dopplerson oscillations decreases significantly, and an additional series of oscillations appears. The theoretical and experimental results are in qualitative agreement. Comparison of the theoretical results with the experimental data leads to the conclusion that the electron-lattice deformation interaction in cadmium predominates over the induction interaction and allows the deformation-interaction constant to be estimated.

PACS numbers: 63.20.-e, 71.85.-a, 72.55.+s

In ^[1-2] it was shown that electromagnetic waves (dopplersons) can propagate in cadmium as a result of the dispersion of the nonlocal conductivity in the vicinity of the Doppler-shifted cyclotron resonance (DSCR). Like helicons, dopplersons are very slow waves: At a frequency of 100 kHz the phase velocity of an electronic dopplerson in cadmium is of the order of 10^3 cm/sec. At higher frequencies the dopplerson velocity becomes comparable to the velocity of sound, which results in the resonance interaction between these waves. In the region of the resonance the attenuation of both waves increases significantly. This dopplerson-phonon resonance is of the same physical nature as the helicon-phonon resonance in metals with different concentrations of electrons and holes. ^[3-5] The influence of the dopplerson on the attenuation of sound in cadmium has been experimentally investigated by Tsybmal and Butenko. ^[6] The present paper is devoted to the study of the properties of dopplerson and sound waves under conditions of their resonance interaction.

1. THEORY

1. The coupling of the dopplerson to the sound wave is due to the interaction of the conduction electrons with the sound and the electromagnetic field. The electric field of the dopplerson gives rise to lattice-ion vibrations; on the other hand, the distortion of the electron distribution function during the propagation of the sound wave leads to the appearance of an electromagnetic field. Mathematically, this is expressed as follows: Into the Maxwell equations enters an extraneous electric current due to the sound wave, while into the lattice-vibration equations enters a force exerted by the electrons on the ions, which is proportional to the electric field of the wave. As a result, the Maxwell equations turn out to be coupled to the lattice-vibration equations. A set of such coupled equations without allowance for the Tolman-Stewart effect was derived in ^[3], and with allowance for this effect in ^[7]. Since under the conditions under consideration by us the indicated effect is negligibly weak, we shall use the simpler equations obtained in ^[3], which equations have the form

$$\text{rot rot } \mathbf{E} = -\frac{4\pi}{c^2} \frac{\partial \mathbf{j}}{\partial t}, \quad (1)$$

$$\rho \frac{\partial^2 u_\alpha}{\partial t^2} = \lambda_{\alpha\beta\gamma\delta} \frac{\partial^2 u_\delta}{\partial x_\beta \partial x_\gamma} + f_\alpha \quad (\alpha, \beta, \gamma, \delta = x, y, z). \quad (2)$$

Here $\mathbf{E}(\mathbf{r}, t)$ is the electric field, $\mathbf{j}(\mathbf{r}, t)$ is the resultant current, $\mathbf{u}(\mathbf{r}, t)$ is the lattice-displacement vector, ρ is the density of the metal, $\lambda_{\alpha\beta\gamma\delta}$ is the elasticity tensor, c is the velocity of light, and f is the volume density of the force exerted by the electrons on the lattice; summation is implied over the repeated vector indices β, γ , and δ .

In the case of a single group of electrons, the current density \mathbf{j} , connected with the propagation of a monochromatic plane wave of frequency ω and wave vector \mathbf{k} is determined by the expression

$$\mathbf{j} = -\frac{2e}{(2\pi\hbar)^3} \int d p_z \frac{m}{\Omega} \int_0^{2\pi} d\varphi v(p_z, \varphi) \int_{-\infty}^{\infty} d\varphi' [\Lambda_{\alpha\beta}(p_z, \varphi') \dot{u}_{\alpha\beta} - e(\mathbf{E} + \mathbf{G})v(\varphi')] \times \exp \frac{1}{\Omega} \int_0^{\varphi'} [v - i\omega + ikv(\varphi'')] d\varphi''. \quad (3)$$

Here e is the absolute magnitude of the electron charge, m is the cyclotron mass, p_z is the component of the momentum \mathbf{p} along the direction of the constant magnetic field \mathbf{H} (the z axis), $\Omega = eH/mc$ is the cyclotron frequency, $\varphi = \Omega t$ is the dimensionless time of electron motion along an orbit in the magnetic field, $v(p_z, \varphi)$ is the velocity on the Fermi surface, ν is the electron-scatterer collision rate, $\Lambda_{\alpha\beta}(\mathbf{p})$ is the deformation-potential tensor characterizing the electron-lattice interaction, $u_{\alpha\beta} = \frac{1}{2}(\partial u_\alpha / \partial x_\beta + \partial u_\beta / \partial x_\alpha)$ is the strain tensor, $\dot{u} \equiv du/dt$, and $\mathbf{G} = c^{-1}[\dot{\mathbf{u}} \times \mathbf{H}]$ is the induced electric field in the system connected with the crystal, a field which arises as a result of the fact that the conductor deformed by the sound wave intersects the lines of force of the magnetic field \mathbf{H} .

In the case of several groups of carriers, the current density \mathbf{j} is a sum of terms of the type (3) corresponding to each group.

The Fourier transforms of the components of the vector \mathbf{j} can be represented in the form

$$j_\alpha = \sigma_{\alpha\beta}(\mathbf{k}, \omega, \mathbf{H})(E_\beta + C_\beta) + j_\alpha^{(A)}, \quad (4)$$

where $\sigma_{\alpha\beta}(\mathbf{k}, \omega, \mathbf{H})$ is the nonlocal-conductivity tensor of the metal and

$$j_a^{(\Lambda)}(\mathbf{k}, \omega, \mathbf{H}) = -\frac{2e}{(2\pi\hbar)^3} \int dp_z \frac{m}{\Omega} \int_0^{2\pi} d\varphi v_a(\varphi) \int_{-\infty}^{\infty} d\varphi' \Lambda_{\beta\gamma}(p_z, \varphi') \dot{u}_{\beta\gamma} \\ \times \exp \left[\frac{v-i\omega}{\Omega} (\varphi' - \varphi) + \frac{i\mathbf{k}}{\Omega} \int_{\varphi}^{\varphi'} v(p_z, \varphi'') d\varphi'' \right]. \quad (5)$$

The vector $\mathbf{j}^{(\Lambda)}$ is the extraneous current due to the interaction of the electrons with the sound wave, $\hat{\sigma}\mathbf{G}$ is the extraneous induced current, while $\hat{\sigma}\mathbf{E}$ is the conduction current; the components of the vector $\hat{\sigma}\mathbf{A}$ are determined by the relation $(\hat{\sigma}\mathbf{A})_{\alpha} = \sigma_{\alpha\beta} A_{\beta}$.

The force \mathbf{f} exerted by the electrons on the lattice also consists of two terms:

$$\mathbf{f} = \frac{1}{c} [\mathbf{j}, \times \mathbf{H}] + \mathbf{f}^{(\Lambda)}, \quad (6)$$

where the first term on the right-hand side is the induction force, while the second is the deformation force.

The Fourier transform of the deformation force, which is connected with the deviation of the electron distribution function from the equilibrium function, is given by the expression

$$j_a^{(\Lambda)}(\mathbf{k}, \mathbf{H}) = ik_{\beta} \frac{2}{(2\pi\hbar)^3} \int dp_z \frac{m}{\Omega} \int_0^{2\pi} d\varphi \Lambda_{\alpha\beta}(p_z, \varphi) \int_{-\infty}^{\infty} d\varphi' [\Lambda_{\gamma\delta}(p_z, \varphi') \dot{u}_{\gamma\delta} \\ - eE\nu(\varphi')] \exp \left\{ \int_{\varphi}^{\varphi'} \frac{v-i\omega + i\mathbf{k}\mathbf{v}(\varphi'')}{\Omega} d\varphi'' \right\}. \quad (7)$$

The first term in the square brackets in (7) causes the sound wave to be damped as a result of the deformation interaction with the electrons. It is not connected with the presence of the doppleron and the electromagnetic field, and has no effect on the doppleron-phonon resonance. Therefore, we shall not consider it. For the same reasons we shall discard part of the induction force, which is proportional to the deformation current $\mathbf{j}^{(\Lambda)}$ and the induced current $\hat{\sigma}\mathbf{G}$.

2. Let us apply the above-presented general relations to the study of the doppleron-phonon resonance in cadmium. Let us consider the propagation of a transverse wave in the case when the wave vector \mathbf{k} and the magnetic field \mathbf{H} are parallel to the hexagonal axis. We shall be interested in the interaction of a sound wave with an electronic doppleron due to the DSCR of the electrons of the "lens." Since the electronic doppleron has a negative circular polarization,^[1] we shall henceforth be interested in only this polarization. Owing to the axial symmetry of the lens about the C_6 axis, the longitudinal electron velocity v_z does not depend on the variable φ , and the expression for the electronic part of the conductivity has the form

$$\sigma_{xx}^{(e)} - i\sigma_{yx}^{(e)} = -i \frac{ec}{H} \frac{2}{(2\pi\hbar)^3} \int_{-p_0}^{p_0} \left(1 - \frac{kc}{2\pi eH} \frac{\partial S}{\partial p_z} - i\gamma \right)^{-1} S(p_z) dp_z, \quad (8)$$

where $S(p_z)$ is the area of the transverse cross section of the lens in the plane $p_z = \text{const}$, $2p_0$ is the thickness of the lens, and $\gamma = \nu/\Omega$; we have neglected the wave frequency ω in comparison with ν . It is convenient to rewrite the formula (8) in the form

$$\sigma_{xx}^{(e)} = -i \frac{ecN(q)}{H(1-i\gamma)}, \quad (9)$$

where

$$q = \frac{kcp_0}{eH(1-i\gamma)}; \quad p_0 = \frac{1}{2\pi} \left. \frac{\partial S}{\partial p_z} \right|_{\text{max}}, \quad (10)$$

and the dependence of N on q is determined by the form of the function $S(p_z)$.

The Doppler-shifted cyclotron resonance of the electrons corresponds to the condition $q = 1$. Since for the holes of the monster, $|\partial S/\partial p_z|_{\text{max}}$ is roughly four times smaller than for the electrons, near the DSCR of the electrons the nonlocal effects in the p-type conductivity are weak and the contribution of the holes to σ_- is well described by the local approximation. The complex form of the monster then has no effect on the form of the conductivity, which depends only on the hole concentration. The total conductivity assumes the form

$$\sigma_-(\mathbf{k}, \mathbf{H}) = -i \frac{ec}{H} \left[\frac{N(q)}{1-i\gamma} - \frac{N(0)}{1+i\gamma_h} \right], \quad (11)$$

where $\gamma_h = \nu_h/\Omega_h$.

In order to compute the deformation current $\mathbf{j}^{(\Lambda)}$ and force $\mathbf{f}^{(\Lambda)}$, we must know the explicit form of the tensor $\Lambda_{\alpha\beta}(\mathbf{p})$. In the case of an isotropic electron dispersion law

$$\Lambda_{\alpha\beta} = Cm \left(v_{\alpha} v_{\beta} - \frac{v^2}{3} \delta_{\alpha\beta} \right), \quad (12)$$

where C is a constant. For metals with anisotropic Fermi surfaces the form of the function $\Lambda_{\alpha\beta}(\mathbf{p})$ is unknown. However, for a qualitative investigation we can assume that also in this case the tensor $\Lambda_{\alpha\beta}$ has the same form. Below we shall assume that $\Lambda_{\alpha\beta}$ is determined by the formula (12).

Let us substitute (12) into (5) and compute the deformation current $\mathbf{j}^{(\Lambda)}$ due to the lens electrons. As a result of simple, but tedious computations, the expression for $\mathbf{j}_-^{(\Lambda)}$ reduces to the form

$$j_-^{(\Lambda)}(\mathbf{k}, \mathbf{H}) = C[N(q) - N(0)] e u_-, \quad (13)$$

where $\mathbf{A}_- = \mathbf{A}_x - i\mathbf{A}_y$.

The deformation current produced by the holes can be neglected in comparison with the electronic current (13). The reason for this is that in the vicinity of the DSCR of the electrons the nonlocal effects in the hole conductivity are very weak, and $N_h(q)$ is close to $N_h(0)$.

The resultant current \mathbf{j} is the sum of the conduction current $\hat{\sigma}\mathbf{E}$, the induced extraneous current $\hat{\sigma}\mathbf{G}$, and the deformation current $\mathbf{j}^{(\Lambda)}$. An analysis shows that the induced current differs from the deformation current only by the absence of the factor C and by small terms of the order of $i\gamma$ and $i\gamma_h$. Neglecting these terms, we can represent the total current \mathbf{j}_- in the form

$$j_- = \sigma_- E_- + (1+C)[N(q) - N(0)] e u_-. \quad (14)$$

Thus, we see that in cadmium the deformation and induced currents turn out to be of the same order of magnitude.

Like the total current \mathbf{j}_- , the force \mathbf{f}_- contains two terms, one of which is proportional to the field \mathbf{E}_- , while the second is proportional to the displacement \mathbf{u}_- . This force is determined by the formula

$$f_-^{(E)} = \frac{1}{c} [(\hat{\sigma}\mathbf{E}) \times \mathbf{H}]_- + f_-^{(\Lambda E)}, \quad (15)$$

where $f_-^{(\Lambda E)}$ is the field part of the force $\mathbf{f}_-^{(\Lambda)}$, which part corresponds to the second term in the square brackets in (7).

To find $f_-^{(\Lambda E)}$, let us substitute (12) into (7) and carry out the integration over φ'' , φ' , and φ . The result can be expressed in terms of the function $N(q)$:

$$f_-^{(\Lambda E)} = C[N(q) - N(0)] e E_-. \quad (16)$$

The computation of the first term on the right-hand side of (15) offers no difficulty. The explicit expression for this term differs from (16) only by the absence of the factor C and by small terms of the order of $i\gamma$ and $i\gamma_h$. Upon neglecting these terms we obtain

$$f_{-}^{(E)} \approx (1+C)[N(q)-N(0)]eE_{-}. \quad (17)$$

Thus, the deformation and induction parts of $f(E)$ are comparable. In this respect, the doppleron-phonon resonance in cadmium differs from the helicon-phonon resonance in uncompensated metals.^[3]

For monochromatic plane waves with negative polarization the set of equations (1)–(2), describing the coupled electromagnetic-acoustic waves, has the form

$$k^2 c^2 E_{-} = 4\pi i \omega j_{-}(k), \quad (k^2 s^2 - \omega^2) u_{-} = \frac{1}{\rho} f_{-}(k), \quad (18)$$

where s is the velocity of transverse sound propagating along the C_6 axis in the absence of a constant magnetic field; $j_{-}(k)$ and $f_{-}(k)$ are the Fourier transforms of the current and force corresponding to the expressions (4) and (6). Neglecting the difference between f_{-} and $f(E)$, and using the formulas (14) and (17), let us write the Eqs. (18) in the form

$$(k^2 c^2 - 4\pi i \omega \sigma_{-}) E_{-} = 4\pi \omega^2 (1+C)[N(q)-N(0)] e u_{-},$$

$$(k^2 s^2 - \omega^2) u_{-} = \frac{1}{\rho} (1+C)[N(q)-N(0)] e E_{-}. \quad (19)$$

The left-hand sides of (19) correspond to noninteracting electromagnetic and sound waves, while the right-hand sides describe their interaction.

The dispersion equation for the coupled waves is obtained from (19) by eliminating u_{-} . Introducing in place of k the dimensionless variable q , (10), and using (11) for σ_{-} , we can represent this equation in the form

$$q^2 - \xi \left\{ \frac{N(q)}{N(0)} - \frac{1-i\gamma}{1+i\gamma_h} \right\} = \frac{\eta \xi^2}{q^2 - q_s^2} \left\{ \frac{N(q)}{N(0)} - 1 \right\} \quad (20)$$

where

$$\xi = \frac{4\pi \omega N(0) p_0^2 c}{e H^2 (1-i\gamma)^3}, \quad q_s = \frac{\omega p_0 c}{e H s (1-i\gamma)}, \quad \eta = \frac{(1+C)^2 H^2 (1-i\gamma)}{4\pi \rho s^2}$$

and $N(q)$ is determined by the relations (8)–(9).

The dimensionless parameter η characterizes the degree of the coupling of the two types of waves. This parameter is small: In a field $H \approx 30$ kOe, the quantity $\eta \approx 10^{-3}$. It follows from this that the sound wave exerts a significant influence on the electromagnetic wave only in the resonance region, where $|q^2 - q_s^2| \ll 1$, and the quantity on the right-hand side of (20) increases.

In order to find the solutions to the dispersion equation, it is necessary to know the explicit form of the function $N(q)$, which depends on the form of the electronic lens. In^[2] a lens model with smooth edges was used which is in good agreement with the results of measurements of the size effect and of the principal properties of the doppleron. Although the corresponding expression for the function $N(q)$ is not very complex, it does not allow an analytic solution of the doppleron dispersion equation. In^[8] a simpler model in which the Fermi surface consists of two paraboloidal cups and a circular cylinder was considered. A modification of this model qualitatively describes all the properties of the electronic doppleron in cadmium^[9] and at the same time allows the determination of the analytic magnetic-field dependence of the

plate impedance in the case of diffuse reflection of the carriers from the surface.^[10] In the present paper we consider the interaction of the electronic doppleron with a sound wave. We use here the paraboloidal model for the electronic lens, and restrict ourselves, in the description of the hole contribution, to the local approximation. In such a model the expression in the curly brackets in (20) has the form

$$\frac{N(q)}{N(0)} - \frac{1-i\gamma}{1+i\gamma_h} \approx \frac{\alpha q^2}{1-q^2} + i(\gamma + \gamma_h), \quad (21)$$

where α is the fraction of the electrons of the paraboloidal cups; it was shown in^[9] that the best agreement with experiment is obtained with $\alpha = 0.4$.

The second term on the right-hand side of (21) determines the small root, proportional to $\sqrt{\gamma + \gamma_h}$ and corresponding to the normal skin effect, of the dispersion equation. Furthermore, this term makes to the damping a contribution that is substantial near the electronic-doppleron threshold, and does not play a role in stronger fields. We are interested in the situation in which the doppleron-phonon resonance occurs at a point appreciably above the doppleron threshold. Under these conditions the skin root

$$q_0 \approx i(\gamma + \gamma_h) \alpha \xi, \quad (22)$$

and its magnitude turns out to be much smaller than the roots, q_1 and q_2 , corresponding to the coupled electromagnetic-sound waves. In such a situation the interaction of the doppleron and the sound wave with the skin component of the electromagnetic field is very weak, and, in determining the roots q_1 and q_2 , the second term on the right-hand side of (21) can be neglected. In other words, the equation for q_1 and q_2 can be represented in the form

$$\left(1 - \frac{\alpha \xi}{1-q^2}\right) (q^2 - q_s^2) = \frac{\eta \xi^2 \alpha^2 q^2}{(1-q^2)^2}. \quad (23)$$

Since the coupling parameter η is very small, the spectrum of the doppleron is, to a first approximation, determined by the relation $1 - q^2 = \alpha \xi$, whose substitution into the right-hand side of (23) leads to the simpler equation

$$\left(1 - \frac{\alpha \xi}{1-q^2}\right) (q^2 - q_s^2) = \eta q^2. \quad (24)$$

This equation describes very well the spectrum of the doppleron and the sound wave in the vicinity of the resonance. The study of the influence of the doppleron on the attenuation of the sound far from the resonance requires the use of (23).

The solution of Eq. (24) offers no difficulty. The corresponding expressions for the wave vectors of the two coupled electromagnetic-sound waves in the region of the resonance are determined by the formulas

$$k_{1,2} = \frac{1}{2} \left(k_{GK}^2 - k_H^2 + \frac{\omega^2}{s^2} \right) \pm \frac{1}{2} \left\{ \left(k_{GK}^2 - k_H^2 - \frac{\omega^2}{s^2} \right)^2 - 2\eta \left[\frac{\omega^2}{s^2} \left(k_{GK}^2 - \frac{\omega^2}{s^2} \right) + k_H^2 (k_{GK}^2 - k_H^2) \right] \right\}^{1/2}, \quad (25)$$

where

$$k_{GK} = -\frac{eH}{p_0 c} (1-i\gamma), \quad k_H^2 = \frac{4\pi \omega \alpha N(0) e}{cH(1-i\gamma)}, \quad (26)$$

k_{GK} is a wave vector characterizing the Gantmakher-Kaner oscillations,^[11] and k_H is the helicon wave vector in the case of a single group of carriers of concentration equal to $\alpha N(0)$.

The root k_1 corresponds to a wave that is primarily electromagnetic, while the root k_2 corresponds to a wave that is primarily acoustic. Without allowance for the interaction with the sound (i.e., for $\alpha \rightarrow 0$), the wave vector of the electromagnetic wave $k^{(0)} = -\sqrt{k_{\text{GK}}^2 - k_{\text{H}}^2}$. The doppleron-phonon resonance occurs upon the coincidence of the wavelengths of the two waves, i.e., at a value of the magnetic field H corresponding to the condition

$$\sqrt{k_{\text{GK}}^2 - k_{\text{H}}^2} = \omega/s. \quad (27)$$

At resonance the first term in the curly brackets in (25) vanishes, and the solution to the dispersion equation can be written in the form

$$k_{1,2} = \mp \frac{\omega}{s} + \frac{i}{2} \left[\sqrt{\eta} k_{\text{H}} \pm \gamma \frac{s}{\omega} \left(k_{\text{GK}}^2 + \frac{k_{\text{H}}^2}{2} \right) \right], \quad (28)$$

where the index r indicates that the quantities η , k_{H} , k_{GK} , and γ , which depend on the magnetic field, should be taken at the value of H corresponding to the resonance (27).

The first term in the square brackets describes the attenuation of the waves as a result of their resonance interaction, while the second term describes the effect of the electron collisions on this attenuation. The expressions (28) are applicable provided the first term is larger than the second. It can be seen that the doppleron attenuation is stronger than the sound-wave attenuation.

The dependence of the real and imaginary parts of k_1 and k_2 on the field H in the vicinity of the resonance is shown in Figs. 1 and 2. The computation was carried out for the values of $f = \omega/2\pi = 50$ MHz, $N(0) = 0.5 \times 10^{22}$ cm $^{-3}$, $\alpha = 0.4$, $p_0 = 1.5\hbar\text{\AA}^{-1}$, $l = v_{\text{F}}/\nu = 0.05$ cm, $C = 1$, and $s = 1.67 \times 10^5$ cm/sec (the value for the velocity, s , of sound was taken from [12]). The resonance manifests itself in some distortion of the spectral curves of both waves and in the appearance of resonance maxima in their attenuation. The increase of $k'' \equiv \text{Im } k_1$ to the left of the resonance is due to the approach to the doppleron threshold, where the doppleron is strongly damped.

Let us now determine the distribution of the electromagnetic field in the metal and the dependence of the plate impedance on the quantity H . The field distribution in the plate in the case of diffuse electron reflection from the surface was investigated in the framework of the paraboloidal model in [10]. The results obtained in [10] can be used for the solution of our problem. In the case under

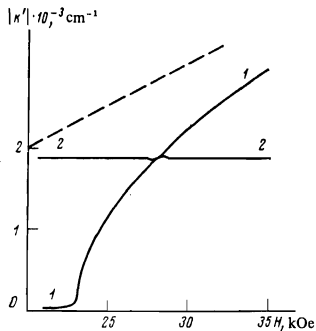


FIG. 1

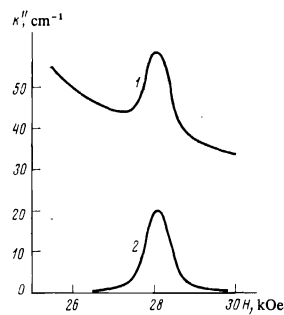


FIG. 2

FIG. 1. The doppleron and sound-wave spectrum in the resonance region (the frequency $f = 50$ MHz).

FIG. 2. Attenuation of the waves in the resonance region at a frequency of 50 MHz: 1) doppleron attenuation; 2) sound-wave attenuation.

consideration the dispersion equation contains two singular terms (poles at the points $k = k_{\text{GK}}$ and $k = \omega/s$) and has three roots: k_0 , k_1 , and k_2 . In this situation the electric-field distribution in a semi-infinite metal $z > 0$ has the form

$$E_-(z) = E_-(0) (a_0 e^{ik_0 z} + a_1 e^{ik_1 z} + a_2 e^{ik_2 z}), \quad (29)$$

where $E_-(0)$ is the electric field on the surface,

$$a_0 = \frac{(k_0 - k_{\text{GK}})(k_0 - \omega/s)(k_2 - k_1)}{k_0^2(k_2 - k_1) + k_1^2(k_0 - k_2) + k_2^2(k_1 - k_0)}, \quad (30)$$

while the expressions for a_1 and a_2 can be obtained from (30) by cyclically permuting the indices. The first term on the right-hand side of (29) is the electric-field component that attenuates in the skin layer, the second term is the doppleron field, and the third term is the electric field due to the sound wave.

The impedance of a plate whose thickness d exceeds the attenuation distances of all the three wave components is determined by the formula [10]

$$Z_-^{(d)} = R_-^{(d)} - iX_-^{(d)} = 2Z_-^{(\infty)} \left[1 - \frac{E_-(d)}{E_-(0)} \right], \quad Z_-^{(\infty)} = \frac{4\pi i \omega}{c^2} \frac{1}{k_0 a_0 + k_1 a_1 + k_2 a_2}$$

is the impedance of the semi-infinite metal; the factor $2Z_-^{(\infty)}$ on the right-hand side takes into account the presence of the two plate surfaces. The second term in the square brackets is due to the penetration of the wave field through the plate; this part of the impedance undergoes oscillations upon the variation of the H field as a result of the variation of the phase of the doppleron propagating through the sample. The results of the computation of the H dependence of the derivative $dR_-^{(d)}/dH$ are shown in Fig. 3. It can be seen that in the resonance region ($H \approx 28$ kOe) the amplitude of the impedance oscillations decreases considerably, while the period increases somewhat. The decrease of the amplitude is due to the rise in the attenuation during the resonance interaction of the waves. The increase, however, of the period is caused by some change in the spectrum of the doppleron.

It should be noted that the impedance oscillations are largely due to the penetration of the doppleron through the plate. The excitation of the sound wave makes some contribution to the impedance only in the resonance region; far from it the electric field of the sound wave, which is proportional to the difference $k_2 - \omega/s$, is negligibly small. The weak sound excitation at resonance is explained by the fact that the phase velocities of the doppleron and sound waves have opposite signs and their interaction turns out to be of little efficacy. Thus, the doppleron-phonon resonance is weaker than the helicon-phonon resonance in the alkali metals. [3-5]

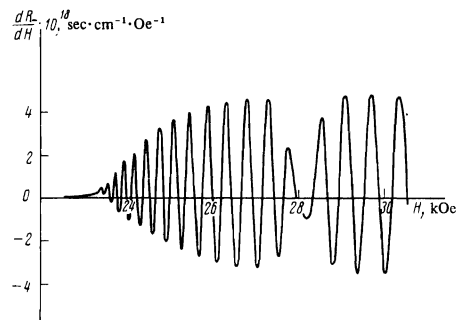


FIG. 3. Plot of the derivative of the surface resistance, dR_-/dH , at a frequency of 50 MHz.

In the helicon-phonon resonance region there exist two series of impedance oscillations corresponding to the excitation of two coupled electromagnetic-sound waves of comparable amplitudes. The doppleron-phonon resonance in cadmium manifests itself primarily as a decrease in the amplitude of the doppleron oscillations as a result of the rise in the doppleron attenuation. An important role is played here by the deformation interaction of the electrons with the sound wave. Without allowance for this interaction, the coupling coefficient η would have been four times smaller and the resonance maximum in the attenuation would have turned out to be so weak that its presence would have virtually had no effect on the impedance oscillations shown in Fig. 3.

2. EXPERIMENT AND DISCUSSION

The experimental study of the doppleron-phonon resonance was carried out on a cadmium plate of thickness $d = 0.57$ mm. The normal to the sample surface coincided to within about one degree with the direction of the hexagonal axis [0001]. The resistance ratio $\rho_{300}/\rho_{4.2K} \approx 3 \times 10^4$. This sample was used earlier for the study of the properties of the doppleron in [9-10].

One of the main experimental difficulties encountered in the observation of the doppleron-phonon resonance consisted in the fact that the doppleron-sound interaction should occur in the region of relatively high frequencies $f > 30$ MHz in strong magnetic fields. The complexity of an experimental investigation in this frequency range is well known. Thus, for example, for the usual autodyne-detector circuits the operating frequency range does not exceed 30-40 MHz. The measurements of the derivative of the surface resistance with respect to the magnetic field were carried out by us with the aid of a specially constructed high-frequency autodyne detector whose upper frequency was limited by the physical feasibility of fabricating oscillatory circuits with lumped inductance and capacitance. The raising of the operating frequency of the autodyne was achieved on account of the application of a generator circuit with a transformer coupling and an optimal matching of the oscillatory circuit and the positive feedback circuit with coaxial cables.

The autodyne circuit is shown in Fig. 4. The master oscillator L_1 and C_1 , in whose induction coil the experimental material is located, is situated in a cryostat and is connected with the grid of the oscillator tube via a separative condenser of small capacitance and a coaxial cable. The positive-feedback signal induced in the coil L_4 is transmitted through the cable to the coil L_2 , which

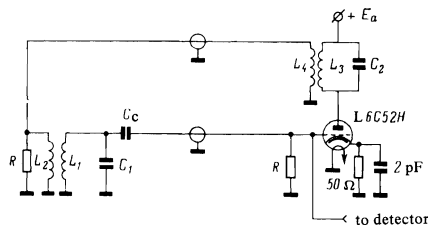


FIG. 4. Circuit diagram of an autodyne for work in the meter band. L_1 and C_1 are the elements of the oscillatory circuit; L_2 and L_4 are coupling coils; L_3 and C_2 are the elements of the anode oscillatory circuit; C_c is a coupling capacitor; the R 's are resistors of resistance equal to the wave impedance of the coaxial cable; E_a is the anode voltage, equal to 50-100 V. The parameters of the indicated elements are chosen with allowance for the operating frequency range.

is inductively coupled with the coil L_1 of the oscillator circuit. Both of the connecting cables terminate on a resistance equal to the wave impedance. In such a wiring scheme the distributed capacitance and inductance of the cables are not introduced into the oscillatory circuit, which allows the operating frequency of the autodyne to be considerably raised.

The excitation of the cadmium plate was effected by a linearly polarized radio-frequency field. The measurement of the surface resistance was carried out in the 25-100 MHz frequency range in a magnetic field produced by a superconducting solenoid. The maximum field of the solenoid was about 65 kOe. The magnetic-field intensity was determined from the solenoid current. The solenoid constant was determined from signals of nuclear magnetic resonance on protons and aluminum nuclei with the aid of the above-described high-frequency autodyne. The nonuniformity of the field did not exceed 0.05%.

In the cadmium surface resistance measurements the coil of the oscillatory circuit together with the experimental material was mounted on a rotatable device that allowed us to rotate the sample in the magnetic field of the solenoid in two mutually perpendicular planes parallel to the direction of the field. At the beginning of each experiment the direction of the magnetic field was set parallel to the hexagonal axis with the aid of the maximum of the doppleron-oscillation amplitude near the doppleron threshold and the symmetry of the $dR/dH(\vartheta)$ curves, where ϑ is the angle between the direction of the field and the axis [0001] of the crystal.

The strict orientation of the magnetic field along the [0001] axis is necessary if the doppleron is not to experience the magnetic Landay damping. As was shown in [13], when the field H deviates from the hexagonal axis this damping leads to a strong attenuation of the doppleron. Under such conditions the doppleron-phonon resonance is highly smeared and difficult to observe.

Examples of the experimental curves of the derivative of the surface resistance of the cadmium plate as a function of the magnetic-field intensity are shown in Fig. 5. The curve in Fig. 5a corresponds to a relatively low frequency, when the doppleron-phonon resonance is shifted towards the region of the doppleron threshold, where, as a result of the strong damping of the wave, the oscillations in the impedance are not observed. The amplitude of the doppleron oscillations in this case increases from the threshold value, attains a maximum, and then smoothly decreases with increasing field intensity. The doppleron-phonon resonance does not appear on this curve. The curves in Fig. 5b were obtained at higher frequencies, at which the resonance occurs significantly above the doppleron threshold. The character of the variation of the oscillation amplitude with the field in these curves differs qualitatively from the behavior of the oscillations in Fig. 5a. At values of $H \approx 27$ kOe the doppleron-oscillation amplitude in the curve 1 of Fig. 5b decreases sharply. Furthermore, in this field region an additional series of oscillations of small amplitude is observed. In the curve 2, obtained at a higher frequency, the decrease of the doppleron-oscillation amplitude occurs in stronger magnetic fields.

The decrease of the oscillation amplitude in the curve 1 of Fig. 5b in the neighborhood of the value $H^1 = 27$ kOe is explained by the rise in the attenuation of the doppleron

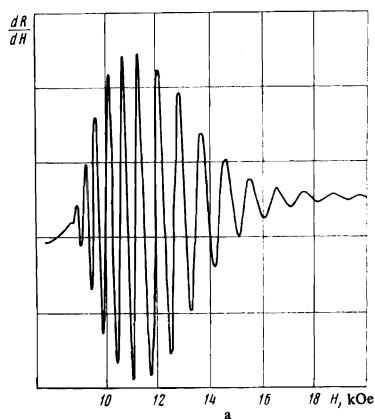
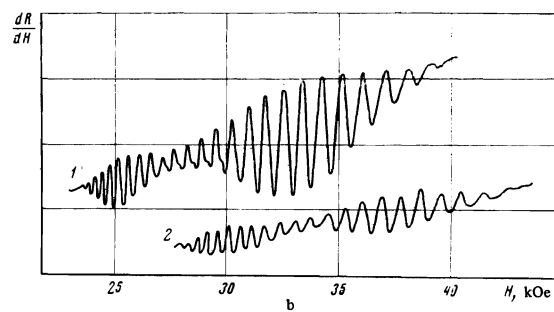


FIG. 5. Recordings of the derivative dR/dH for a cadmium plate located in a magnetic field at $T = 1.5$ K and at different frequencies: a) $f = 3$ MHz; b) for the curve 1, $f = 50$ MHz and for the curve 2, $f = 73$ MHz.



as a result of its resonance interaction with the sound wave (see the curve 1 in Fig. 2). The physical cause of the decrease of the oscillations in the impedance in the resonance region consists in the conversion of part of the electromagnetic energy of the doppleron into acoustic-oscillation energy.

The observed location of the doppleron-phonon resonance agrees with the theoretical value, H_R , obtainable from Eq. (27). Thus, at a frequency of 50 MHz experiment gives the value $H_R = 27$ kOe, while the theory gives $H_R = 28$ kOe. At a frequency of 73 MHz (the curve 2 in Fig. 5b) the experimental value for $H_R = 34$ kOe, while the theoretical value is 35 kOe.

Comparison of the curve 1 in Fig. 5b with the theoretical curve in Fig. 3 shows that the results of the theory are in qualitative agreement with experiment. It is difficult to expect complete quantitative agreement of the theory with experiment, since the considered model for the Fermi surface of cadmium is a crude approximation to the real Fermi surface. The primary difference between the experimental and theoretical results consists in the fact that in the theory the doppleron-phonon resonance is weaker. The decrease of the oscillation amplitude in the curve 1 of Fig. 5b occurs in a wider field region and is more drastic than in the theoretical curve. The computation was carried out for an electron mean free path $l = 0.5$ mm. If we take a shorter mean free path, then the resonance region broadens slightly, but the oscillation attenuation at resonance turns out to be less significant. For better agreement of the theory with experiment, it is necessary to increase the electromagnetic wave-sound wave coupling factor. The induction interaction does not contain unknown parameters, and we cannot change its magnitude. On the other hand, the magnitude of the deformation interaction, which is characterized by the parameter C , can, in principle, be increased. The experimental results indicate that the quantity C exceeds unity and has the value $C \approx 2-4$. The

larger value of C is also attested by the presence of the series of additional oscillations in the curve 1 of Fig. 5b. These oscillations are due to the dispersion of the sound-wave velocity in the resonance region. However, for the value $C = 1$ this dispersion is so weak (see Fig. 1) that it does not lead to additional oscillations in the impedance as a function of the magnetic field. Accordingly, such oscillations are absent in the curve in Fig. 3.

Thus, we can infer that the doppleron-phonon resonance in cadmium is largely determined by the electron-sound deformation interaction, and not by the induction interaction. In this respect, the resonance in cadmium differs from the helicon-phonon resonance in uncompensated metals, in which the induction interaction is not weakened as a result of compensation.

The present paper is devoted, in the main, to the study of the doppleron-phonon resonance in the case when the magnetic field H is oriented parallel to the hexagonal axis of the crystal. Let us now briefly discuss the question of the effect on the resonance of the deviation of the vector H from the [0001] axis. As was noted above, when the vector H is not parallel to this axis, there arises Landau damping, which weakens the doppleron-sound interaction. Besides this obvious effect, the inclination of the magnetic field to the axis leads to a considerable shift in the location of the resonance towards the region of strong fields. In Fig. 6 we show recordings demonstrating the variation of the resonance value of the field as the angle ϑ between the vector H and the [0001] axis is varied. It can be seen that the resonance shift is quite large: for $\vartheta = 0.5^\circ$ the quantity H_R increases by 2.9 kOe, while for $\vartheta = 1^\circ$ it increases by 4.4 kOe. It might have been assumed that such a resonance shift is due to a change in the doppleron spectrum upon the deviation of the vector H from the hexagonal axis. However, this assumption contradicts the results of the study of doppleron propagation in an inclined magnetic field.^[13] Another possible explanation could have been that the appearance of the Landau damping shifts the resonance, as occurs in an oscillatory circuit when its Q -factor is changed. Unfortunately, this assumption also does not allow the explanation of the observed resonance shift, the nature of which remains unclear.

In conclusion, let us say a few words about the relation between the obtained results and Tsymbal and Butenko's data.^[6] In the present paper we have studied the

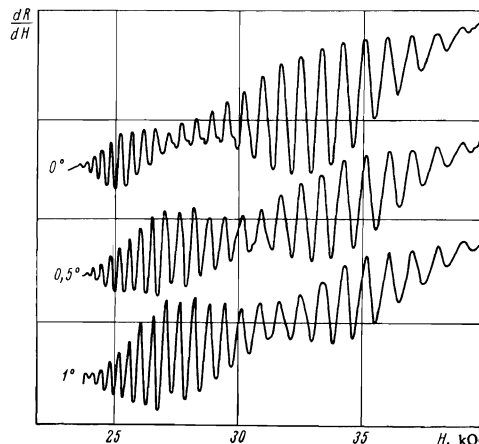


FIG. 6. Recordings of the derivative dR/dH for different angles ϑ . $T = 1.5$ K.

effect of the doppleron-phonon resonance primarily on the electromagnetic properties of cadmium, while in ^[6] the effect on the absorption of sound was studied. There is some discrepancy between the results of these investigations. According to our results, the attenuation of the electromagnetic and sound waves has maxima in the region of their resonance interaction. In contrast, the anomaly in the absorption of sound, observed in ^[6], is more of a jump than a maximum. The authors are grateful to V. G. Fastovskii for his attention to the work.

¹L. M. Fisher, V. V. Lavrova, V. A. Yudin, O. V. Konstantinov, and V. G. Skobov, Zh. Eksp. Teor. Fiz. **60**, 759 (1971) [Sov. Phys.-JETP **33**, 410 (1971)].

²O. V. Konstantinov, V. G. Skobov, V. V. Lavrova, L. M. Fisher, and V. A. Yudin, Zh. Eksp. Teor. Fiz. **63**, 224 (1972) [Sov. Phys.-JETP **36**, 118 (1973)].

³V. G. Skobov and É. A. Kaner, Zh. Eksp. Teor. Fiz. **46**, 273 (1964) [Sov. Phys.-JETP **19**, 189 (1964)].

⁴C. C. Grimes and S. J. Buchsbaum, Phys. Rev. Lett. **12**, 357 (1964).

⁵A. Libchaber and C. C. Grimes, Phys. Rev. **178**, 1145 (1969).

⁶T. L. Tsybal and T. F. Butenko, Solid State Commun. **13**, 633 (1973).

⁷V. M. Kontorovich, Zh. Eksp. Teor. Fiz. **45**, 1638 (1963) [Sov. Phys.-JETP **18**, 1125 (1964)].

⁸R. G. Chambers and V. G. Skobov, J. Phys. **F1**, 202 (1971).

⁹V. V. Lavrova, S. V. Medvedev, V. G. Skobov, L. M. Fisher, and V. A. Yudin, Zh. Eksp. Teor. Fiz. **64**, 1839 (1973) [Sov. Phys.-JETP **37**, 929 (1973)].

¹⁰V. V. Lavrova, S. V. Medvedev, V. G. Skobov, L. M. Fisher, and V. A. Yudin, Zh. Eksp. Teor. Fiz. **65**, 705 (1973) [Sov. Phys.-JETP **38**, 349 (1974)].

¹¹V. F. Gantmakher and É. A. Kaner, Zh. Eksp. Teor. Fiz. **48**, 1571 (1965) [Sov. Phys. JETP **21**, 1053 (1965)].

¹²C. W. Garland and J. Silverman, Phys. Rev. **119**, 1218 (1960).

¹³V. V. Lavrova, V. G. Skobov, L. M. Fisher, A. S. Chernov, and V. A. Yudin, Fiz. Tverd. Tela **15**, 2335 (1973) [Sov. Phys.-Solid State **15**, 1558 (1974)].

Translated by A. K. Agyei
244